POLITECNICO DI TORINO
Repository ISTITUZIONALE

Measurement Technique for the Permanent Magnet Rotor Thermal Time Constant Determination

(Article begins on next page)

20 January 2022

Measurement Technique for the Permanent Magnet Rotor Thermal Time Constant Determination

Eric Armando
Dipartimento Energia "G.Ferraris"
Politecnico di Torino
Torino, Italy
eric.armando@polito.it

Aldo Boglietti
Dipartimento Energia "G.Ferraris"
Politecnico di Torino
Torino, Italy
aldo.boglietti@polito.it

Salvatore Musumeci
Dipartimento Energia "G.Ferraris"
Politecnico di Torino
Torino, Italy
salvatore.musumeci@polito.it

Sandro Rubino
Dipartimento Energia "G.Ferraris"
Politecnico di Torino
Torino, Italy
sandro.rubino@polito.it

Enrico Carpaneto
Dipartimento Energia "G.Ferraris"
Politecnico di Torino
Torino, Italy
enrico.carpaneto@polito.it

Daniele Martinello
Dipartimento Energia "G.Ferraris"
Politecnico di Torino
Torino, Italy
daniele.martinello@polito.it

Abstract—**In this paper, an innovative measurement technique that allows the determination of the permanent magnet thermal time constant of permanent magnet synchronous machines is proposed. The novelty of the proposed procedure consists of the determination of the permanent magnet thermal time constant without the test being influenced by the other rotor parts such as lamination, shaft, etc. Therefore, it can be applied to any permanent magnet synchronous machine type, assuming general validity. The proposed experimental setup consists of controlling the currents of the machine under test while an external electric drive sets its speed. Experimental results for two permanent magnet synchronous machine types are presented, demonstrating the feasibility of the proposed procedure.**

Keywords—thermal time constant, permanent magnet synchronous machines, thermal analysis.

I. INTRODUCTION

Over the last years, following the needs of the market, the development of high-performance electric drives has known impressive growth. Indeed, based on modern applications like electric and hybrid vehicles [1], [2], railway traction, servomotors for machine tools, strong overload capability of the drive is often required. However, this feature leads to the strong thermal stress of the electrical machine, making mandatory the thermal modeling of this latter.

From the thermal point of view, it is well-known how the stator windings are the most critical part of the machine. However, in the case of permanent magnet synchronous machines (PMSM) are considered, the thermal behavior of the magnets must also be taken into account. This analysis becomes mandatory mainly when a strong overload operation of the machine is performed, leading at the reaching of its thermal limits. In this condition, because the magnetic properties of the magnets are thermal-sensitive [3], the performance of the electric drive could result in compromised [4]. This condition is further emphasized in PMSMs characterized by a magneto-motive force on the air gap with high harmonic content.

It is known how an increase of the permanent magnet (PM) temperature can cause a not negligible drop of the related flux density, leading to a reduction of the torque production capability. In extreme cases, the magnets could be demagnetized irreversibly, putting the electrical machine out of order. For this reason, together with the thermal sensors used for monitoring the stator windings (e.g., thermocouples), modern electric drives usually include a simplified thermal model of the machine.

In this way, it is possible to perform the estimation of both stator windings and PM temperature [5]-[8]. However, accurate thermal parameters must be used in the model. As a consequence, these must be measured properly. The stator winding thermal resistance and thermal capacitance can be easily measured using a short transient thermal test, as proposed and discussed by the authors in [9], [10].

Regarding the PM thermal parameters, these are not easy to measure because the PM is not an independent thermal source like the stator windings. As a consequence, the PM thermal parameters cannot be measured without the presence of other motor losses [11], [12], hindering their evaluation with high accuracy.

To solve this issue, an innovative measurement technique for determining the PM thermal time constant is proposed in this paper. The main advantage of the proposed procedure consists of the accuracy of the result, together with the possibility of real-time monitoring of the transient of both stator windings temperature and PM flux density. The measurement technique is deeply analyzed, along with the full description of the experimental setup. Experimental results are provided for two low-power PMSMs, demonstrating the validity of the proposed method.

The paper is organized as follows. The descriptions of both the experimental setup and the proposed test procedure are reported in Section II e III, respectively. The data-processing for the computation of the PM thermal time constant is given in Section IV. Experimental test results are shown in Section V. Additional remarks are reported in Section VI while Section VII concludes the paper.

II. EXPERIMENTAL SETUP

The experimental setup for the determination of the PM thermal time constant is like that used for the identification of the flux linkage maps of synchronous ac motors [13], [14], as shown in Fig. 1.

The shaft of the motor under test (MUT) is mechanically coupled to a driving machine (DM) acting as a prime mover. If the procedure for the identification of flux linkage maps is performed, a torque sensor along to the mechanical connection between MUT and DM is mounted. However, for the determination of the PM thermal time constant, the torque measurement is not needed, allowing the direct connection between MUT and DM. Regarding the control of these, the DM is speed-controlled while the MUT is current-controlled, using a current vector control (CVC) scheme implemented in the physical (d,q) frame.
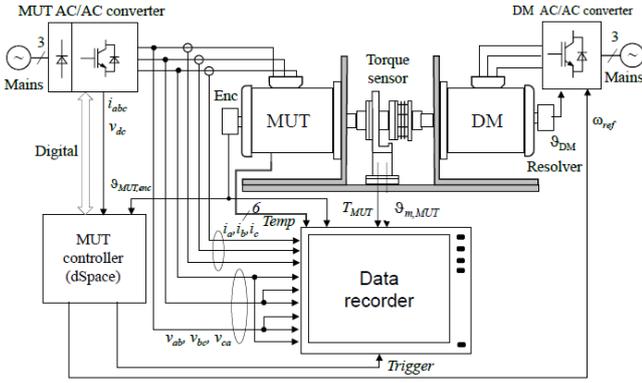
Fig. 1.   Test rig for the PM thermal time constant determination [15].

Fig. 2.   Variation of the *d*-axis current in each thermal point [14].

Therefore, the rotor position is measured using a mechanical sensor (e.g., encoder). Alternatively, the torque sensor could be employed for the position measurement, as shown in Fig. 1. Indeed, some commercial torque sensors can provide the feedback on mechanical position together with that of the torque.

Concerning the electrical feedback, both phase voltages and phase currents of the MUT are measured. The measurement of the phase currents is necessary to perform the CVC algorithm, using the digital controller interfaced with the inverter that feeds the MUT (Fig. 1). However, for the evaluation of the PM thermal time constant, the phase voltages measurement must be performed.

The phase voltages measurement can be performed in several ways. A cheap solution consists of reconstructing the phase voltages from the inverter duty-cycle commands, together with the measurement of the dc-link voltage. However, if specific data recorders are employed [15], the line-to-line voltages of the MUT can be measured directly, using high-voltage/high-speed acquisition channels. In this way, the pulse width modulation (PWM) voltages applied by the inverter are properly acquired, allowing the reconstruction of the time-fundamental phase voltages, as shown in Fig. 1.

If a data recorder is employed, all measurements can be stored on it. In this case, both mechanical (torque, position) and electrical (voltage and currents) feedback are received by the instrument, as shown in Fig. 1.

Concerning the control of the DM, it can consist of an industrial electric drive that receives the reference speed command by the digital controller, as shown in Fig. 1. Additional details are not reported because they are beyond the scope of the work.

III.   Test Procedure

The proposed test procedure consists of heating the MUT to get the temperature time-evolution of both stator windings and PM. The duration of the heating test depends on the overall thermal time constant of the MUT. Indeed, it is necessary to inject current on the MUT until the steady-state thermal condition is reached. Therefore, the proposed procedure can require 30-60 minutes for very small machines up to several hours for bigger ones.

During the machine heating, the temperatures of the stator windings and PM are indirectly evaluated, using the measurements of the stator winding resistance and PM flux linkage.
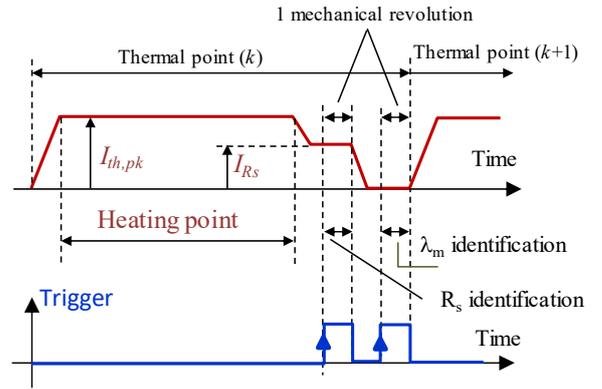
Since the goal of this procedure is to get the time-evolutions of these two variables, the heating procedure is structured in a predefined number of thermal points. In each thermal point, both the machine heating and identification of stator resistance and PM flux linkage are performed.

The duration of each thermal point depends on the time-resolution with which to represent the time-evolution of the two above mentioned variables. Usually, the duration of each thermal point is chosen in the range of 2-5 minutes, depending on the duration of the heating procedure.

For example, by heating the MUT for 3 hours (180 minutes) and by setting the duration of each thermal point at 2 minutes, an overall number of 90 thermal points (180/2) is performed. Therefore, the time-evolutions of both stator resistance and PM flux linkage will be represented by 90 measurement points.

The heating procedure consists of applying a predefined (*d*,*q*) current vector on the MUT, using the CVC scheme. The *q*-axis current component is set at zero to avoid the machine torque production. Concerning the *d*-axis current component, this is set at a value $I_{th,pk}$ such to inject the RMS thermal current $I_{th,rms}$ ($I_{th,pk}/I_{th,rm} = \sqrt{2}$). A reasonable choice is to set the thermal current value equal to MUT rated current.

The variation of the *d*-axis current in each thermal point is shown in Fig. 2. It is noted how, after the machine heating, the *d*-axis current component is set at a value I_{Rs} such to perform the stator winding resistance identification. This value can be chosen arbitrarily. It can also correspond with the thermal current value. However, to avoid further heating of the MUT, it is recommended to choose a lower value.

Finally, the PM flux linkage identification is performed. This value is estimated through the measurement of the PM-induced back-electromotive-force (emf). Therefore, during the PM flux linkage identification, the *d*-axis current component is set at zero. To guarantee the generation of the PM-induced back-emf, the MUT must be driven by the DM at a constant target speed. This value should be limited to avoid relevant MUT's iron losses generated by the PM on the stator core.

The identifications of stator winding resistance and PM flux linkage are performed indirectly, using the measurements of phase currents, phase voltages, and mechanical position.

In conclusion, to better understand the proposed test procedure, the main steps of this can be summarized as follows:

1) To limit the iron losses, the MUT is driven by DM at a constant low-speed value, anyway able to guarantee the proper sensing of the PM-induced back-emf.

2) The MUT is current-controlled, using a CVC scheme implemented in the physical (d,q) frame. Only the d-axis current component is controlled at a value different from zero. Conversely, the q-axis current component is set at zero, avoiding the MUT torque production.

3) The heating procedure is structured into several thermal points, which number depends on their time-length an on the overall time to guarantee the steady-state thermal condition of the MUT.

4) The d-axis current variation during each thermal point follows the profile shown in Fig. 2. After the machine heating, the identification of stator winding resistance and PM flux linkage is performed, using the measurements of phase voltages, phase currents, and mechanical position.

5) At the procedure end, all measurements collected by the data recorder (or in the alternative by the digital controller used to control the MUT) are elaborated to get the profile of stator winding resistance and PM flux linkage.

A. Identification of the stator winding resistance

The identification of the stator winding resistance is performed using the d-axis voltage and current components. These are obtained starting from the measurements of phase voltages and phase currents. Indeed, by using the measured mechanical position, the Park transformation is applied, leading to the computation of the (d,q) variables.

To mitigate the effects of the MUT's stator slots, the d-axis voltage and current components are computed as an average of all values sampled in one mechanical revolution. Therefore, by denoting with V_d and I_d the respective d-axis average voltage and current components, the stator winding resistance value R_s at the generic thermal point k is computed as:

$$R_s(k) = \frac{V_d(k)}{I_d(k)} \cong \frac{V_d(k)}{I_{R_s}} \tag{1}$$

Since the d-axis current is controlled at the value I_{Rs} by the CVC scheme, the approximation made in (1) is justified. Once the stator winding resistance is evaluated, the average stator winding temperature T_s at the generic thermal point k is computed as:

$$T_s(k) = \frac{R_s(k)}{R_0} \cdot (234.5 + T_0) - 234.5 \tag{2}$$

where R_0 is the stator winding resistance at the initial test temperature T_0, usually correspondent with that of the external environment, while 234.5 is the copper temperature coefficient.

B. Identification of the PM flux linkage

Since the identification of the PM flux linkage is performed in zero-current condition (ensured by the CVC scheme), the phase voltages of the MUT represent the PM-induced back-emf. Therefore, by using the measured mechanical position, the Park transformation is applied, leading to the computation of the (d,q) back-emf voltages.

Together with these, also the mechanical speed of the MUT is necessary, computed by starting from the mechanical position measurement.

Finally, to mitigate the effects of the MUT's stator slots, the (d,q) back-emf voltages and mechanical speed are computed as an average of all values sampled in one mechanical revolution. Therefore, by denoting with V_q and ω_m the respective q-axis average voltage component and mechanical speed, the PM flux linkage λ_m at the generic thermal point k is computed as:

$$\lambda_m(k) = \frac{V_q(k)}{p \cdot \omega_m(k)} \tag{3}$$

where p stands for the pole-pairs number of the MUT. Finally, to convert the variables (1)-(3) from the sampled-time domain to the continuous-time one, it is necessary to introduce the time length Δt of each thermal point, leading to as follows:

$$X(t) = X(k \cdot \Delta t) \tag{4}$$

where X represents the generic variable of resistance, temperature, or flux. As a consequence, the time-variations of the PM flux linkage are available, allowing the determination of the related thermal time constant.

IV. PM THERMAL TIME CONSTANT COMPUTATION

Once the time-evolutions of the stator winding resistance, stator winding temperature, and PM flux linkage have been obtained, it is possible to compute the time constants associated with these. Based on the goal of this paper, the computation of the PM thermal time constant is emphasized.

According to experimental results that will be shown in the next section, the time-evolution of the PM flux linkage can be described by a first-order time-differential model, having a solution described by the following time-equation:

$$\lambda_m(t) = a + (b-a) \cdot e^{-\frac{t}{c}} \tag{5}$$

The coefficients (5) can be computed using several fitting methods. However, in this paper, to provide a physical interpretation of (5), an empirical method based on the following assumptions is used:

$$\begin{cases} a = \lambda_m(t \to \infty) \\ b = \lambda_m(t = 0) \\ c = \tau_m \end{cases} \tag{6}$$

where:

- $\lambda_m(t = 0)$ is the PM flux linkage at the starting time instant of the heating procedure;

- $\lambda_m(t \to \infty)$ is the PM flux linkage at the end of the heating procedure, corresponding to the steady-state thermal condition of the MUT;

- τ_m is the PM thermal time constant, consisting of the primary goal of this work.

The computation of the PM thermal time constant can be performed by minimizing the sum of the squares of the errors between (5)-(6) and experimental time-evolution obtained with (4), using a conventional spreadsheet.

Similarly, with a right level of approximation, also the time-evolution of the stator winding resistance/temperature can be described by a first-order time-differential model, having a solution described by the following time-equation:

$$
\begin{cases}
R_s(t) = R_0 + \left[R_s(t \to \infty) - R_0 \right] \cdot \left(1 - e^{-\frac{t}{\tau_s}} \right) \\
T_s(t) = T_0 + \left[T_s(t \to \infty) - T_0 \right] \cdot \left(1 - e^{-\frac{t}{\tau_s}} \right)
\end{cases}
\tag{7}
$$

where:

- $R_s(t \to \infty)$ is the stator winding resistance at the end of the heating procedure, corresponding to the stator winding temperature $T_s(t \to \infty)$;

- τ_s can be considered an overall thermal time constant of the MUT, corresponding to a mix of all the time constants that characterize the thermal path between the stator winding and the external environment.

Like the previous case, the computation of the overall thermal time constant of the MUT can be performed by minimizing the sum of the squares of the errors between (7) and experimental time-evolutions obtained with (4).

V. EXPERIMENTAL TEST RESULTS

The experimental validation of the proposed measurement technique has been carried out on two PMSMs, both rated 600 W. The first, from now onwards called MUT_1, is a fractional-slot surface permanent magnet (SPM) machine having 36 poles. The second machine, from now onwards called MUT_2, is a spoke-rotor interior permanent machine (IPM) having 8 poles. The main features of both machines are reported in Table I.

A. Test Rig

The reference speed of the DM has been set at 100 r/m and 300 r/m for MUT_1 and MUT_2, respectively.

The inverter consists of a three-phase insulated gate bipolar transistor (IGBT) power module fed by a bidirectional dc source. The switching frequency has been set at 16 kHz.

The digital controller is the dSPACE® DS1103 fast prototyping board while the CVC algorithm has been developed in the C-code environment. The sampling frequency has been set at 16 kHz.

The data recorder consists of the Gen3i from HBM Gmbh, equipped with two high voltage cards GN610 (± 1kV input, each card has six differential channels with a sample rate of 2 MS/s, 18 bit for a channel), for line-to-line voltages and phase currents measurements.

B. Experimental results for MUT_1

The time-evolutions of PM flux linkage and stator winding temperature for the MUT_1 are shown in Figs. 3 - 4. It is noted how both stator winding and PM are in steady-state thermal condition, with a thermal time constant of 32 min and 44 min, respectively.

The steady-state stator winding temperature is near to 100.5 °C with, a related PM flux linkage drop of about 5.9 %, demonstrating a strong temperature-independent behavior.

TABLE I. MAIN DATA OF THE MACHINES UNDER TEST

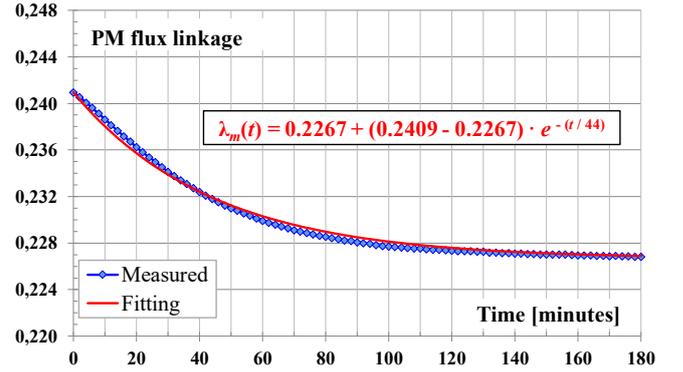| -	MUT_1	MUT_2
Rotor Type	SPM – Outer Rotor	IPM – Spoke Rotor
Winding Type	Concentrated	Concentrated
Poles number	36	8
Rated power	600 W	600 W
Rated speed	1600 r/m	3000 r/m
Rated voltage	220 Vrms	190 Vrms
Rated current	5 Arms	2.75 Arms
PM flux linkage	241 mVs	76.4 mVs

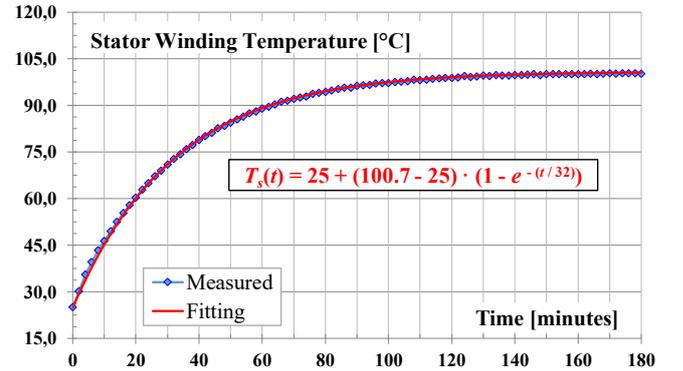Fig. 3. Time-evolution of the PM flux linkage for MUT_1.

Fig. 4. Time-evolution of the stator winding temperature for MUT_1.

The experimental results demonstrate how both the time-evolutions of PM flux linkage and stator winding temperature can be described using a first-order model, allowing the definition of a single thermal time constant for each of them.

C. Experimental results for MUT_2

The time-evolutions of PM flux linkage and stator winding temperature for the MUT_2 are shown in Figs. 5 - 6. It is noted how, also in this case, both stator winding and PM are in steady-state thermal condition, with a thermal time constant of 36 min and 48 min, respectively.

The steady-state stator winding temperature is near to 132.6 °C with, a related PM flux linkage drop of about 24.7 %, demonstrating a very strong temperature-dependent behavior (unlike MUT_1).
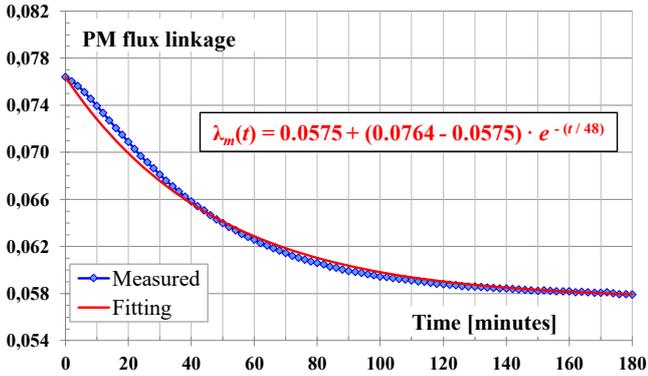
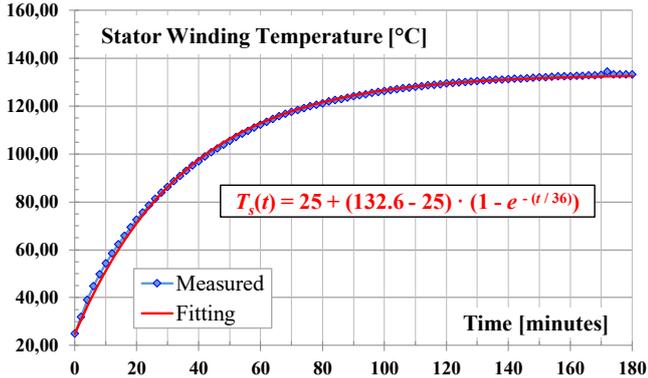Fig. 5. Time-evolution of the PM flux linkage for MUT_2.

In the figure:
$$\lambda_m(t) = 0.0575 + (0.0764 - 0.0575) \cdot e^{-(t/48)}$$

Fig. 6. Time-evolution of the stator winding temperature for MUT_2.

In the figure:
$$T_s(t) = 25 + (132.6 - 25) \cdot (1 - e^{-(t/36)})$$

TABLE II.   Main Data of the Machines Under Test

-	MUT_1	MUT_2
Initial stator winding temperature	25 °C	25°C
Final stator winding temperature	100.7 °C	132.6 °C
Overall thermal time constant	32 min	36 min
Initial PM flux linkage	240.9 mVs	76.4 mVs
Final PM flux linkage	226.7 mVs	57.5 mVs
PM flux linkage drop	5.9 %	24.7 %
PM thermal time constant	44 min	48 min

Like the previous case, the experimental results demonstrate how both the time-evolutions of PM flux linkage and stator winding temperature can be described using a first-order model. Therefore, the use of a single time constant to represent the time-evolution of the PM temperature is justified. Finally, in Table II are summarized the results obtained for both MUTs.

VI. Final Remarks

The presented activity should be considered as a preliminary approach to the measurement and the identification of the PM thermal parameters employed in PMSMs. Indeed, the proposed procedure allows at obtaining the PM thermal time constant. However, it is not possible to extrapolate the values of PM thermal resistance R_{th-m} and PM thermal capacitance C_{th-m}.

Since the PMs are warmed by the stator winding losses, the heat must cross the machine air-gap before to reach them. As known, the air thermal conductivity is very high compared to the thermal conductivity of the other materials involved in the heat transfer. As a consequence, approximately, the thermal resistance due to the air-gap can be considered the only active during the test. Therefore, if the geometrical data of the air-gap are known, the PM thermal resistance R_{th-m} can be computed as [16]:

$$R_{th-m} = \frac{1}{2\pi \cdot k_{air} \cdot L_s} \cdot \ln\left(\frac{r_{is}}{r_{is} - l_{ag}}\right) \quad (8)$$

where r_{is} is the inner stator radius, l_{ag} is the air-gap thickness, k_{air} is the air thermal conductivity while L_s is the lamination length. Therefore, the PM thermal capacitance C_{th-m} can be computed using the PM thermal time constant as follows:

$$C_{th-m} = \frac{\tau_m}{R_{th-m}} \quad (9)$$

Nevertheless, since the geometrical dimensions of the machines used for the experimental validation are not still available, the PM thermal parameters cannot be computed, thus representing the future development of this work.

VII. Conclusion

The paper proposes an innovative measurement technique for the determination of the permanent magnet thermal time constant. The proposed test procedure consists of heating the machine to get the temperature time-evolutions of both stator windings and permanent magnet. The experimental setup is like that used for the identification of the flux linkage maps of synchronous ac motors. Based on the obtained experimental results, the time-evolution of the permanent magnet temperature can be described by a first-order time-differential model, allowing the definition of a single thermal time constant. Experimental results for two permanent magnet synchronous machines have been presented, providing the validation of the proposed method.

References

[1] Z. Q. Zhu and D. Howe, "Electrical Machines and Drives for Electric, Hybrid, and Fuel Cell Vehicles," in *Proceedings of the IEEE*, vol. 95, no. 4, pp. 746-765, April 2007.

[2] I. Boldea, L. N. Tutelea, L. Parsa and D. Dorrell, "Automotive Electric Propulsion Systems With Reduced or No Permanent Magnets: An Overview," in *IEEE Transactions on Industrial Electronics*, vol. 61, no. 10, pp. 5696-5711, Oct. 2014.

[3] T. Sebastian, "Temperature effects on torque production and efficiency of PM motors using NdFeB magnets," in *IEEE Transactions on Industry Applications*, vol. 31, no. 2, pp. 353-357, March-April 1995.

[4] S. Li, D. Han and B. Sarlioglu, "Analysis of the influence of temperature variation on performance of flux-switching permanent magnet machines for traction applications," 2017 IEEE International Electric Machines and Drives Conference (IEMDC), Miami, FL, 2017, pp. 1-6.

[5] G. D. Demetriades, H. Z. d. l. Parra, E. Andersson and H. Olsson, "A Real-Time Thermal Model of a Permanent-Magnet Synchronous Motor," in *IEEE Transactions on Power Electronics*, vol. 25, no. 2, pp. 463-474, Feb. 2010.

[6] C. Kral, A. Haumer and S. B. Lee, "A Practical Thermal Model for the Estimation of Permanent Magnet and Stator Winding Temperatures," in *IEEE Transactions on Power Electronics*, vol. 29, no. 1, pp. 455-464, Jan. 2014.

[7] D. D. Reigosa, D. Fernandez, T. Tanimoto, T. Kato and F. Briz, "Permanent-Magnet Temperature Distribution Estimation in Permanent-Magnet Synchronous Machines Using Back Electromotive Force Harmonics," in *IEEE Transactions on Industry Applications*, vol. 52, no. 4, pp. 3093-3103, July-Aug. 2016.

[8] D. Park, H. Jung, H. Cho and S. Sul, "Design of Wireless Temperature Monitoring System for Measurement of Magnet Temperature of IPMSM," 2018 IEEE Transportation Electrification Conference and Expo (ITEC), Long Beach, CA, 2018, pp. 656-661.

[9] A. Boglietti, E. Carpaneto, M. Cossale and S. Vaschetto, "Stator-Winding Thermal Models for Short-Time Thermal Transients: Definition and Validation," in *IEEE Transactions on Industrial Electronics*, vol. 63, no. 5, pp. 2713-2721, May 2016.

[10] A. Boglietti, M. Cossale, S. Vaschetto and T. Dutra, "Winding Thermal Model for Short-Time Transient: Experimental Validation in Operative Conditions," in *IEEE Transactions on Industry Applications*, vol. 54, no. 2, pp. 1312-1319, March-April 2018.

[11] M. Ganchev, C. Kral, H. Oberguggenberger and T. Wolbank, "Sensorless rotor temperature estimation of permanent magnet synchronous motor," IECON 2011 - 37th Annual Conference of the IEEE Industrial Electronics Society, Melbourne, VIC, 2011, pp. 2018-2023.

[12] M. Ganchev, C. Kral and T. Wolbank, "Compensation of speed dependency in sensorless rotor temperature estimation for permanent magnet synchronous motor," 2012 XXth International Conference on Electrical Machines, Marseille, 2012, pp. 1612-1618.

[13] E. Armando, R. I. Bojoi, P. Guglielmi, G. Pellegrino and M. Pastorelli, "Experimental Identification of the Magnetic Model of Synchronous Machines," in *IEEE Transactions on Industry Applications*, vol. 49, no. 5, pp. 2116-2125, Sept.-Oct. 2013.

[14] E. Armando, P. Guglielmi, G. Pellegrino and R. Bojoi, "Flux linkage maps identification of synchronous AC motors under controlled thermal conditions," 2017 IEEE International Electric Machines and Drives Conference (IEMDC), Miami, FL, 2017, pp. 1-8.

[15] R. Bojoi, E. Armando, M. Pastorelli and K. Lang, "Efficiency and loss mapping of AC motors using advanced testing tools," 2016 XXII International Conference on Electrical Machines (ICEM), Lausanne, 2016, pp. 1043-1049.

[16] A. Boglietti, A. Cavagnino, M. Lazzari and M. Pastorelli, "A simplified thermal model for variable-speed self-cooled industrial induction motor," in *IEEE Transactions on Industry Applications*, vol. 39, no. 4, pp. 945-952, July-Aug. 2003.